

## Additive Manufacturing of Anatomical Phantoms Based on Medical Imaging Data Sets

Fabian KLINK\*<sup>1</sup>, Thomas HOFFMANN\*<sup>2</sup>, Axel BOESE\*<sup>3</sup>,  
Martin SKALEJ\*<sup>4</sup> and Karl-H. GROTE\*<sup>5</sup>

\*1, 5 Department of Machine Design, University of Magdeburg  
Universitätsplatz 2, 39106 Magdeburg, GERMANY  
fabian.klink@ovgu.de, karl.grote@ovgu.de

\*2, 3, 4 Department of Neuroradiology, University of Magdeburg  
Leipziger Str. 44, 39120 Magdeburg, GERMANY  
t.hoffmann@ovgu.de, axel.boese@ovgu.de, martin.skalej@med.ovgu.de

### Abstract

Over the last years the use of anatomic phantoms has steadily increased in medicine and medical engineering. These models are helpful for medical training, but also for treatment planning of scheduled surgical interventions and for testing of newly developed techniques, respectively. For the production of anatomic phantoms, medical images can be used. These data usually consist 2D-images taken from magnetic resonance imaging (MRI) or computed tomography (CT). By reconstruction, it is possible to generate 3D-volume data sets. These are the basics for segmentation of single structures and manufacturing e.g. by rapid prototyping (RP). Depending on the qualitative demands, the generation of anatomical phantoms can be achieved by different RP methods.

**Keywords:** rapid prototyping, reverse engineering, segmentation, anatomical phantom

### 1 Introduction

The worldwide use of rapid prototyping technologies steadily increases. The continuous improvement of RP-systems in quality and speed of manufacturing allows the creation of reliable products such as models of anatomical structures in adequate time [1]. These models can be used as demonstrational or educational objects especially for training surgeons or for preparing specific interventions. In medical engineering, the models are useful tools for validation and testing during the product development process. Each RP model consists of thin stacked up layers. This production technique allows the creation of complex undercuts which are not easily feasible with conventional manufacturing. Some RP-processes (for example stereolithographic manufacturing) allow the manufacturing of inner structures and even cavities. Hereby it is possible to reproduce hollow sections like a vessel system or spongiform structures of the bones. The potential of RP technologies in combination with medical imaging as a reverse engineering approach will be described in this publication using as an example the surgical X-ray head phantom. The flowchart in **Fig. 1** shows the different steps to generate an anatomic phantom based on medical imaging data sets.

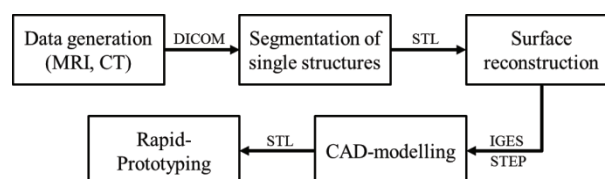
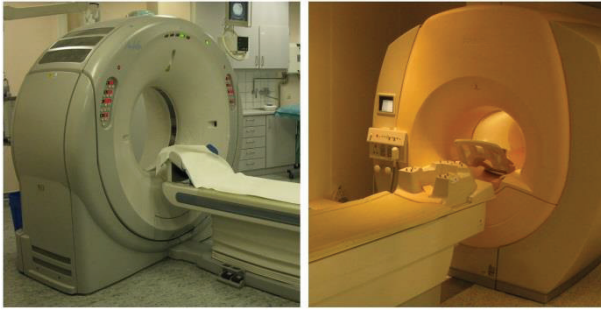


**Fig. 1 Workflow to generate an anatomic phantom (Squares show process stages, arrows the file format of exported data sets)**

### 2 Data generation

Anatomically correct phantoms are based on medical data sets from the various medical imaging procedures, e.g. image sets of patients or dissected structures obtained by MRI, X-ray or CT systems. The University of Magdeburg is equipped with the respective systems for patient care, research and education purposes. For the acquisition of CT-datasets, a 16 slice CT scanner (Toshiba Aquilion 16, Toshiba Medical Systems, Toshigi, Japan) is available (see **Fig. 2**, (a)). This scanner delivers fast image acquisition and high spatial resolution. In CT systems, an X-ray source rotating around the patient creates a set of projections. These can be reconstructed in a 2D image by reconstruction algorithms (filtered back projection). By moving the patient through the X-ray beam a stack of images can be acquired. Depending on the X-ray density of the scanned object, the gray value of the resulting image is changing. Thus, dense structures like the outer cortical bone and soft tissue or ligaments can be differentiated. By aid of these systems it was possible to investigate a tumor (meningioma) of the inner meninges situated above a patient's left eye. A contrast enhanced CT-angiography (CTA) of the head was performed to visualize the tumor vascularization using the contrast agent Imeron 300 (Bracco Imaging, Milano, Italy).

A second data set from the same patient was acquired by MRI (Philips Intera 1.5T, Philips Health Care, Best, Netherlands) (see **Fig. 2**, (b)). MRI allows the differentiation of anatomical structures and is especially suitable to image soft tissue. The MRI technique is based on the content of hydrogen-atoms within the scanned object. Thereby, a differentiation of



(a) CT-scanner Toshiba Aquilion 16 (b) MRI-scanner Philips Intera 1.5T

Fig. 2 Medical imaging data sets

Table 1 Characteristic values of the CT and MRI data sets

	CT data set (head, tumor, arteries)	MRI data set (brain)
Image size	512 x 512 pixel	512 x 512 pixel
Pixel size	0.47 x 0.47 mm <sup>2</sup>	0.43 x 0.43 mm <sup>2</sup>
Image distance	0.4 mm	0.43 mm
Number of images	561	350
File size	290 MB	175 MB

anatomical structures is feasible. For diagnostics of the tumor and its influence on the surrounding brain tissue a sense sequence (ST1 3H HR) was applied.

To create a surgical X-ray head phantom, the CTA and MRI data sets of the patient were picked up for the further reverse engineering process. The data sets (see Table 1) were acquired in DICOM format, a broadly accepted standard format containing aside the diagnostic images additional information about the scanning process [2].

### 3 Data processing

#### 3.1 Segmentation

For adaptation of the images and preparation for generative manufacturing, the MRI and CT data sets have to be converted into a suitable data format [3]. For that purpose, the digital image is segmented into associated regions by combination of adjacent pixels whereby the gray values of the medical images can be utilized to characterize soft tissues and bone structures within the MRI or CT data (see Fig. 3, [4]). This allows the segmentation of anatomical structures by different image processing methods (threshold method, masking, morphologic filter, region growing, contour detection). For image processing the open source software MeVisLab (MeVis Medical Solution AG, Fraunhofer MeVis) was used.

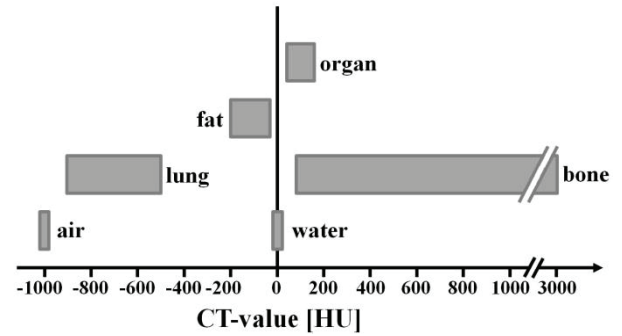
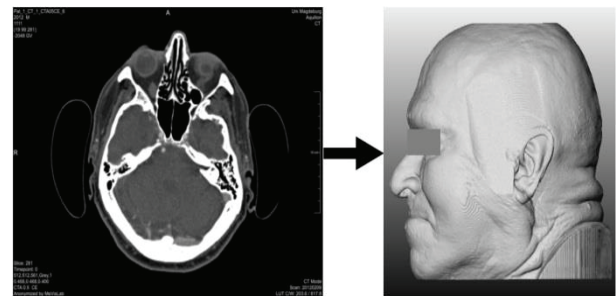


Fig. 3 Gray values of different structures in CT images, adapted from [4]

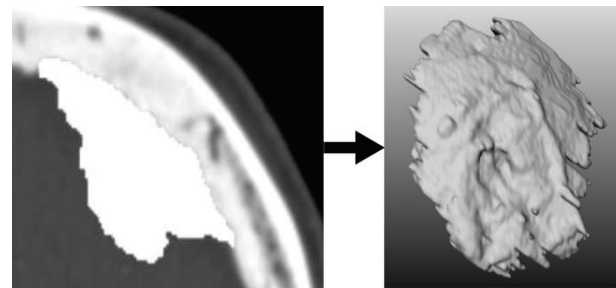
The outer contour of the head phantom is segmented from the images of the CT data set. This allows separation of skin and bone structures from the surrounding air. For a more convenient CAD-modeling (computer-aided design), the head is segmented as a filled object and will be eroded by aid of spline volumes during the following CAD process. This creates the environment for the inner anatomical structures like the brain, the arteries and the tumor. Potential air-containing cavities such as nose or ear are filled and thus will appear as solid structures. Figure 4 is a visualization of the head data set. The shape of the head fixation during imaging is still visible. Using the CT data set a segmentation of the tumor could be performed (see Fig. 5). Tumor calcification allowed the identification of the tumor and its distinction from the surrounding tissues and bones.



(a) Input CT data set

(b) 3D visualization of the head

Fig. 4 Segmented and 3D visualized head of the patient



(a) Masked tumor region data set

(b) 3D visualization of the tumor

Fig. 5 Segmented and 3D visualized tumor structure

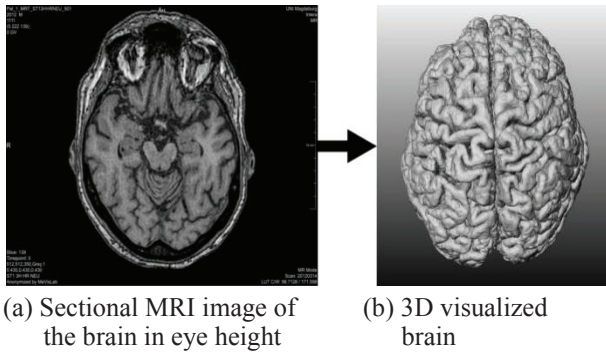


**Fig. 6 Segmented and visualized brain**

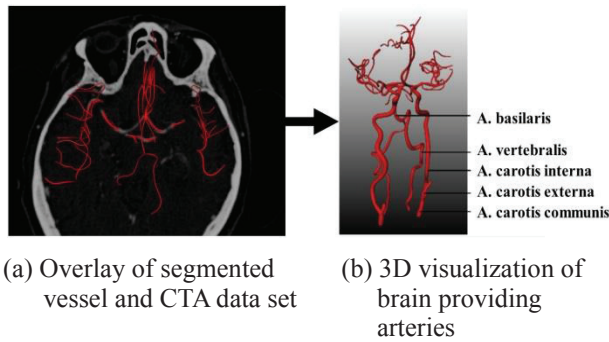


**Fig. 7 Segmented and visualized arteries**

Segmentation and visualization of the brain were achieved from the MRI data set. MRI delivers excellent contrast of soft tissue which facilitates the brain segmentation process. For MRI data sets, the same segmentation procedures as mentioned above for CT were operated. In areas with closely attached structures of similar gray values (e.g. in the eyes region) a threshold segmentation is not possible which makes the manual selection and subtraction of the structures necessary. Small holes within inner parts of the brain are closed by morphologic filtering (see **Fig. 6**).

To segment the arterial system, the data processing is performed on contrast enhanced CTA-images (see **Fig. 7**). The contrast agent fills up the inner vessel structure during the imaging procedure. Thus, a pronouncedly higher gray value of the vessel tree can be achieved which allows threshold segmentation. Minor arterial branches sometimes cannot be distinguished from the skull bones. Thus, for semi-automatic segmentation manual detachment of these arteries is necessary.

### 3.2 Mesh optimization

After segmentation the data sets are transformed into polygon meshes and the surface is optimized. Occurring errors of the mesh are cleared and potential holes closed. Depending on the mesh quality, the surface has to be smoothed to remove buckles derived from direct voxel transformation. During this step, loss of details has to be considered. As a difference to geometrically constructed objects, the resulting surface consists of more radii and bends. A very fine meshing of the polygons is necessary to achieve detailed rendering. The resulting data sets consist of very large files (300-700 MB). By using decimation algorithms it is possible to subtract about 70% of the polygons without

decisive loss of quality. Parts with a large number of bends are netted finer than parts with plain surfaces. This results in smaller file sizes (50-120 MB) to facilitate further processes. Automatic surface reconstruction was performed using the software Geomagic Studio 12 (Geomagic Inc., United States). Additional surface optimization, algorithms for error analysis and mending tools are implemented. Every segmented data set (head, brain, tumor, arteries) is loaded into the program and processed. After the automatic NURBS-retransition it is possible to generate parametric surfaces which can be processed in CAD-programs to create and edit volume models.

### 3.3 CAD modeling

To gain an anatomically correct position of the segmented structures, the coordinate systems of the data sets have to be transformed uniformly (registration). The CT-coordinate system is the basis for the coordinate system in the CAD program. Here, the segmentation of tumor, head and arteries is already at the right position. Alignment of the brain is performed by identifying anatomical reference points. In order to ascertain congruency of the reference points, the brain is manually registered.

The anatomical structures of the planned head phantom should be removable to improve the visibility for demonstration purposes (see **Fig. 8**). To allow the removal of parts of the phantom, adding drillings and bolts within the CAD-modeling were required. The skull cap was detached and separated into two pieces to allow collision free removal of the brain. The brain itself is divided into left and right hemisphere with a cut through the brainstem. A connection of the hemispheres is enabled by three drillings and appropriated pins. With small boards a connection to the head is possible. The brain supplying arteries (left and right internal carotid artery, left and right vertebral artery) are also divided into right and left hemisphere. Provided with matching surfaces and connecting-pins, these parts can be fixed at the right position inside the phantom.

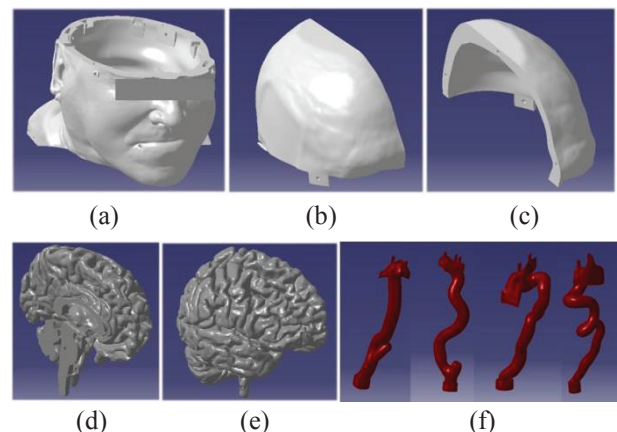


**Fig. 8 (a) Lower part of the head with retaining boards, (b) Right part of the head, (c) Left part of the head, (d) Left hemisphere, (e) Right hemisphere, (f) Main brain providing arteries (Arteria vertebralis, Arteria carotis)**



## 4 Generative production

For the production of the head phantom different techniques were applied. The tumor tissue was generated with vacuum casting inside of an RP-printed casting mold. The lower head contour was also produced by RP and fitted with a transparent silicon filling. For the manufacturing of head, skullcap, brain, arteries and the connection elements RP-techniques were used. The selected printing method depended on the required production quality, an X-ray contrast of the material suitable for imaging, and the overall material and building costs.

The head contour with left and right cranium was generated using ZPRINTER 310 (3D Systems Inc., Rock Hill, United States) (see **Fig. 9**, (a)). This RP-technology - also known as 3D printing - coats single layers of powder with a binder sprayed by a nozzle to connect the layers. An infiltration with superglue (Z-Bond™ 90 Infiltrant, 3D Systems Inc.) after manufacturing and a sintering process additionally hardened the resulting 3D model [5]. The maximum possible size of the model, limited by the printer, is 203 x 254 x 203 mm<sup>3</sup> with a layer density of 0.089 mm to 0.203 mm. The tensile and bend load of the printed elements is very poor due to the used material. Because of occurring deviations, the fitting surfaces need to be post-processed. By achievement of the required X-ray contrast and the comparatively low material costs, this method provides the optimal technology for the manufacturing of the outer head phantom.

For the right and left hemispheres of the brain, a manufacturing process with optimal accuracy is required. In addition, the arteries of the phantom should be hollow and without support structures. The RP process stereolithography was used for manufacturing of the brain and the brain supplying arteries. Within this process the layers of the virtual model were drawn by a UV-laser in a photo polymeric liquid bath. The building platform is lowered as predefined after each layer and is re-wetted uniformly with a wiper. Free hanging surfaces are protected with additionally generated support structures which have to be manually removed after the building process [6]. The photo polymeric liquid VisiJet® Tough (3D Systems Inc.) which due to its viscosity allows construction of cavities up to 5 mm in diameter and exposed overhangs up to 3 mm without additional support structures was used. Thus, the production of arterial cavities is possible. The stereolithography system ProJet® 6000 (see **Fig. 9**, (b)) from 3D Systems Inc. is offering a potential model size of 250 x 250 x 250 mm<sup>3</sup> and provides a minimal layer density of 0.05 mm.

**Figure 10** shows the resulting head phantom. Due to the modular construction, an assembly in different variants is possible. In the lower part of the head the large arteries leading to the brain are embedded in silicon created by vacuum casting. The two cerebral hemispheres are connected by pins and secured with retaining boards on the head. These parts can be removed separately. The vacuum casting mold for the tumor was printed with ZPrinter® 310. The tumor can be attached by pins at the left half of the brain.



(a) 3D printer ZPrinter® 310 (b) Stereolithographic system ProJet® 6000

**Fig. 9 Rapid Prototyping systems**

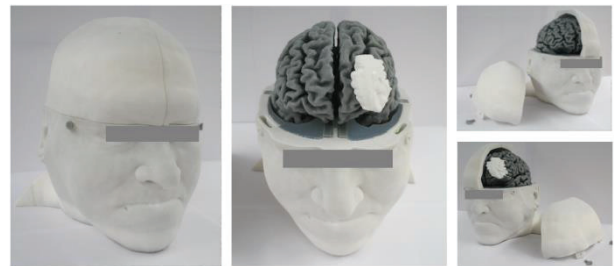
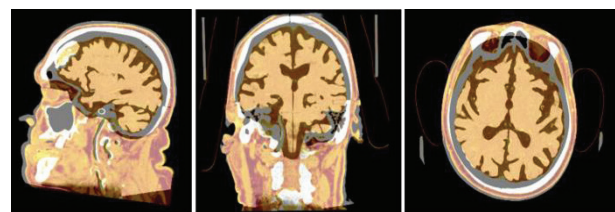


**Fig. 10 Developed head phantom in different configurations**

## 5 Verification

For validation of the alignment of the brain, tumor, and the arteries within the head contour, the original CT data were overlaid by a CT image set of the manufactured phantom (see **Fig. 11**). The deviations range below 0.5 mm. Only the position of the tumor and a small gap between the brain hemispheres may lead to minimal differences. Overall, the model meets the requirements of a surgical head phantom.



(a) Sagittal view (b) Frontal view (c) Transversal view

**Fig. 11 Phantom data sets (dark) in overlay of original data set (light)**

## 6 Conclusions

It is possible to produce an anatomically correct head phantom based on medical imaging data sets. Images of a real patient MRI and CT scans could be processed using segmentation, 3D visualization and

surface reconstruction to produce CAD compatible data sets. Segmentation could be performed using various image processing methods and workflows referring to state of the art techniques. Different parts of the head including the brain, arteries and a tumor could be processed separately. The file size of the complex data sets could be reduced successfully. In the context of CAD modeling the alignment in a uniform coordinate system of the MRI and CT data sets was performed. A CAD modeling of the anatomical structures by adding drillings and fitting boards was possible. As a result, a CAD model with 26 parts was developed. For each part, a specific manufacturing method was assigned depending on the respective requirements. Hereby, the special characteristics in material and quality of the different RP systems have to be focused.

### Acknowledgments

The work of this paper is partly funded by the German Ministry of Education and Research (BMBF) within the Forschungscampus STIMULATE under grant number '03FO16101A' and '03FO16102A'.

### References

- [1] Pahl, G.; Beitz, W.; Feldhusen, J., Grote, K.-H.: Konstruktionslehre: Grundlagen erfolgreicher Produktentwicklung, Methoden und Anwendung. Berlin, Springer-Verlag, (2007), Chap. 13, pp.743-749 – ISBN 978-3-540-34060-7.
- [2] Dugas, M.; Schmidt, K.: Medizinische Informatik und Bioinformatik. Berlin, Springer-Verlag, (2003), Chap. 3, pp.94-96 – ISBN 978-354-042568-7.
- [3] Berger, U.; Hartmann, A.; Schmid, D.: Additive Fertigungsverfahren: Rapid Prototyping, Rapid Tooling, Rapid Manufacturing. Haan-Gruiten, Verlag Europa-Lehrmittel, (2013), Chap. 5, pp.154-161 – ISBN 978-3-8085-5033-5.
- [4] Akadhi, H.; Leschka, S.; Stolzmann, P.; Scheffel, H.: Wie funktioniert CT? Berlin, Springer-Verlag, (2011), Chap. 1, pp.4-13 – ISBN 978-3-642-17802-3.
- [5] Hoyer, J.; Uhl, C.; Beyer, C.: Fortschritt-Berichte VDI Nr. 656 Virtual & Rapid Prototyping. Düsseldorf, VDI Verlag, (2006), Chap. 5, pp.61-87 – ISBN 3-18-365602-7.
- [6] Gebhardt, A.: Generative Fertigungsverfahren: Rapid Prototyping – Rapid Tooling – Rapid Manufacturing. München, Carl Hanser Verlag, (2013), Chap. 3, pp.101-115 – ISBN 978-3-446-43652-0.
- [1] Pahl, G.; Beitz, W.; Feldhusen, J., Grote, K.-H.: Konstruktionslehre: Grundlagen erfolgreicher Produktentwicklung, Methoden und Anwendung. Received on October 10, 2013  
Accepted on January 22, 2014